Universal Unfolding of Pitchfork Bifurcations and Shear-Band Formation in Rapid Granular Couette Flow *

Meheboob Alam

Engineering Mechanics Unit, Jawaharlal Nehru Center for Advanced Scientific Research, Jakkur P.O., Bangalore 560064, India; Email: meheboob@jncasr.ac.in

Abstract. A numerical bifurcation analysis is carried out to understand the role of gravity on the shear-band formation in rapid granular Couette flow. At *low* shear rates, there is a unique solution with a *plug* near the bottom wall and a *shear-layer* near the top-wall; this solution mirrors typical shearbanding-type profiles in earth-bound shear-cell experiments. Interestingly, a *stable* plug near the top-wall is also a solution of these equations at *high* shear rates; there is a multitude of other plugged states, with the plugs being located in an ordered fashion within the Couette gap. The origin of such shearbanding solutions is tied to the spontaneous symmetry-breaking *shearbanding* instabilities of the gravity-free uniform shear flow, leading to both subcritical and supercritical pitchfork bifurcations. In the language of singularity theory, we have established that this bifurcation problem admits *universal unfolding* of pitchfork bifurcations.

1   Introduction

Granular materials (e.g. sand, coal, cereals, powders, etc.) are of immense importance in many industrial and geological processes; most agricultural and pharmaceutical products are in granular form. The motion of a collection of macroscopic solid particles represents a granular flow [7,5] as in a vibrofluidized bed. The external driving is essential to sustain such flows since the particle collisions are inherently dissipative, leading to a 'continual' energy loss. Thus, granular flows represent a *driven-nonequilibrium* system. In typical 'dry' granular flows, the effect of interstitial fluid is neglected and the interactions between grains are *dissipative*, which, in turn, leads to a wealth of interesting behaviour [7,5]. Despite their practical importance and non-trivial dynamics, the current understanding of granular flows still remains at its infancy.

Over the last two decades, the computer simulation studies on granular shear flows have unveiled many interesting dynamical features (such as cluster-formation, density-waves, plug formation, stress-fluctuations, etc.) of such flows [8,9]. These studies have subsequently stimulated many works on the associated macroscopic flows described by suitable continuum equations. One major goal of these theoretical works has been to test the available continuum models from the viewpoint of predicting such pattern-formation in the rapid shear regime. To this end, the kinetic-theory constitutive models [12,1,2] have been routinely used. The general concensus that appears to have emerged is that the Navier-Stokes-level constitutive models are able to explain many interesting dynamical states of such rapid-shear flows. We remark here that the non-Newtonian rheology is also important for granular fluids [7,3], but theoretical works with non-Newtonian constitutive models are still lacking.

In the present paper, we have performed linear instability and bifurcation analyses of the granular Couette flow under gravity using a kinetic-theory-based Newtonian hydrodynamic

---

* Proceedings of the Symposium on Trends in Applications of Mathematics to Mechanics, 22-28 August 2004, Seeheim, Germany (Editors: K. Hutter and Y. Wang; Shaker Verlag)

model. Along with a synthesis of some recent work [4], here we provide new results on the effect of gravity on subcritical bifurcations which firmly establish a link between our results and the singularity theory of bifurcations. We have shown that the origin of *shear-band* formation in such flows is tied to an instability of the associated 'gravity-free' uniform shear flow via the route of the universal unfolding of pitchfork bifurcations.

2   Hydrodynamic Model: Plane Couette Flow

The hydrodynamic model that we have employed is based on the kinetic theory of inelastic hard-spheres [7]. Under the assumption of instantaneous binary collisions, the kinetic theory provides a set of hydrodynamic equations for the density $\tilde{\rho} = \tilde{\rho}_p \nu$, the hydrodynamic velocity $\tilde{\boldsymbol{u}}$ and the granular energy $\tilde{T}$, where ν is the volume fraction of particles and $\tilde{\rho}_p$ is their intrinsic density. Note that the granular temperature is an additional (*higher-order*) field variable, defined via $\tilde{T} = <\delta \tilde{\boldsymbol{u}}^2/3>$ where $\delta \tilde{\boldsymbol{u}}$ is the fluctuation velocity of a particle over the mean motion. At the Navier-Stokes order, the hydrodynamic equations

$$\left(\frac{\partial}{\partial t} + \tilde{\boldsymbol{u}} \cdot \tilde{\nabla} \right) \tilde{\rho} = -\tilde{\rho} \nabla \cdot \tilde{\boldsymbol{u}}, \tag{1a}$$

$$\tilde{\rho} \left(\frac{\partial}{\partial t} + \tilde{\boldsymbol{u}} \cdot \tilde{\nabla} \right) \tilde{\boldsymbol{u}} = -\tilde{\nabla} \cdot \tilde{\boldsymbol{\Sigma}} + \tilde{\rho} \tilde{\boldsymbol{g}}, \tag{1b}$$

$$\frac{3}{2} \tilde{\rho} \left(\frac{\partial}{\partial t} + \tilde{\boldsymbol{u}} \cdot \tilde{\nabla} \right) \tilde{T} = -\tilde{\nabla} \cdot \tilde{\boldsymbol{q}} - \tilde{\boldsymbol{\Sigma}} : \tilde{\nabla} \tilde{\boldsymbol{u}} - \tilde{\mathcal{D}}, \tag{1c}$$

represent the mass, momentum and energy balances, respectively. Here $\tilde{\boldsymbol{\Sigma}}$ is the stress tensor, $\tilde{\boldsymbol{q}}$ the energy-flux, $\tilde{\boldsymbol{\Sigma}} : \tilde{\nabla} \tilde{\boldsymbol{u}}$ the production of fluctuation energy due to shear-work, $\tilde{\mathcal{D}}$ the rate of collisional dissipation of fluctuation energy and $\tilde{\boldsymbol{g}}$ is the acceleration due to gravity. Note that the collisional dissipation rate vanishes identically for perfectly elastic collisions (i.e. the coefficient of restitution is $e = 1$). As mentioned, the third equation is a balance for the fluctuation kinetic energy which is needed since the transport properties of granular fluids depend on the granular temperature. We employ the standard Newtonian constitutive model of an inelastic dense gas for the stress tensor $\tilde{\boldsymbol{\Sigma}}$, the energy flux $\tilde{\boldsymbol{q}}$ and the collisional dissipation rate $\tilde{\mathcal{D}}$ as detailed in [10].

   The plane Couette flow under gravity, as shown schematically in Fig. 1, is driven by two oppositely-moving walls at $\tilde{y} = -\tilde{H}/2$ and $\tilde{y} = \tilde{H}/2$. In the Cartesian coordinate system, $\tilde{u}(x, y, t)$ and $\tilde{v}(x, y, t)$ denote the streamwise and transverse velocity components in the $\tilde{x}$- and $\tilde{y}$-directions, respectively. Using the separation between the two walls $\tilde{H}$ as the length scale, the velocity difference between the walls $\tilde{U}_w$ as the velocity scale and the inverse of the overall shear rate $\tilde{H}/\tilde{U}_w = \tilde{\gamma}^{-1}$ as the time scale, one can obtain the non-dimensional equations of motion in terms of dynamical variables ν, $\boldsymbol{u} = (u, v)$ and T [4]. With this non-dimensionalization procedure, the top and bottom walls move with velocities $\pm 1/2$, respectively.

   For the steady ($\partial/\partial t = 0$), fully developed ($\partial/\partial x = 0$) plane Couette flow under gravity, the mass balance equation is identically satisfied. The x-momentum, y-momentum and energy balance equations reduce to

$$\frac{\mathrm{d}}{\mathrm{d}y} \left(\mu \frac{\mathrm{d}u}{\mathrm{d}y} \right) = 0, \tag{2a}$$

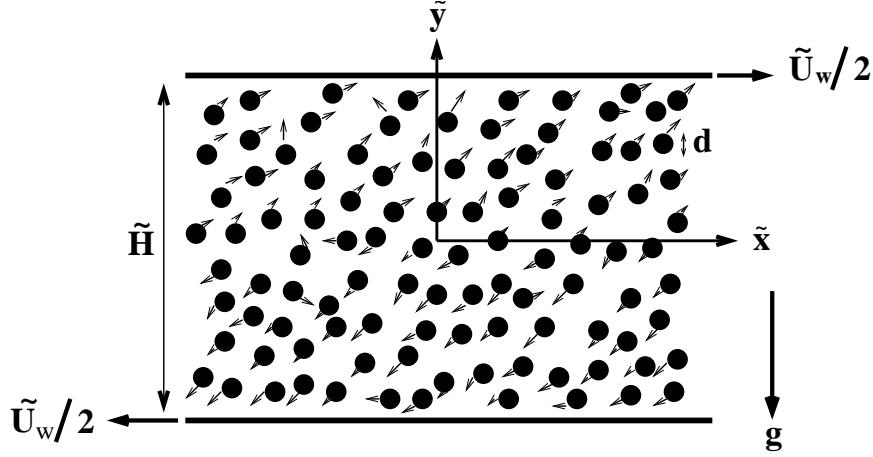**Fig. 1.** A schematic of the plane Couette flow of monodisperse granular materials, with the particle size being $\tilde{d}$

$$\frac{\mathrm{d}p}{\mathrm{d}y} + \frac{\nu H^3}{Fr^2} = 0, \tag{2b}$$

$$H^{-2}\frac{\mathrm{d}}{\mathrm{d}y}\left(\kappa\frac{\mathrm{d}T}{\mathrm{d}y}\right) + \mu\left(\frac{\mathrm{d}u}{\mathrm{d}y}\right)^2 - \mathcal{D} = 0, \tag{2c}$$

respectively. Here $p(\nu, T) = f_1(\nu, e)T$, $\mu(\nu, T) = f_2(\nu, e)\sqrt{T}$, $\kappa(\nu, T) = f_4(\nu, e)\sqrt{T}$ and $\mathcal{D}(\nu, T) = f_5(\nu, e)T^{3/2}$ are the nondimensional forms of the pressure, shear viscosity, pseudo-thermal conductivity and the collisional dissipations, respectively. The explicit forms for these non-dimensional functions $f_1 - f_5$ are detailed elsewhere [1].

Only four non-dimensional control parameters are needed to describe the present problem: the average solid fraction ν_{av}, the non-dimensional Couette gap $H = \tilde{H}/\tilde{d}$, the co-efficient of restitution e, and the Froude number $Fr = \tilde{U}_w/\sqrt{\tilde{g}\tilde{d}}$ (or, the non-dimensional weighted shear rate). Note that $Fr = \gamma\tau_d$ can be written as a ratio between two time-scales, where $\gamma = \tilde{U}_w/\tilde{H}$ is the external shear rate and $\tau_d = H(\tilde{d}/\tilde{g})^{1/2}$ is the gravitational time scale. The case of zero-gravity (i.e. $g = 0$) corresponds to $Fr^{-1} = 0$ which can also be recovered by considering the infinite shear-rate limit ($\gamma \to \infty$).

For all our calculations, we have adopted the *no-slip* and *zero* energy-flux boundary conditions. (The effects of slip-velocity and non-zero energy-flux do not introduce any new physics [1,11,4] since the reported shear-band formation is driven by a bulk-instability.) With these ideal boundary conditions, the gravity-free case admits a uniform shear solution with constant solid fraction and granular energy:

$$\nu(y) = \text{const.} , \quad u(y) = y, \quad T(y) = f_2(\nu, e)/f_5(\nu, e). \tag{3}$$

It is easy to verify that equations (2a–2c) with $Fr^{-1} = 0$ admit the following symmetry:

$$\nu(y) = \nu(-y), \quad u(y) = -u(-y), \quad T(y) = T(-y). \tag{4}$$

i.e. the solid fraction and granular temperature are symmetric about the mid-plane ($y = 0$), and the velocity is antisymmetric for the uniform shear flow. However, for the plane Couette flow with gravity ($Fr^{-1} \neq 0$), this *center-symmetry* is no longer preserved.

3   Shear-banding Instability: Sub- and Supercritical Pitchfork Bifurcations

For instability analysis, the uniform shear flow is perturbed by infinitesimal perturbations, viz.,

$$\nu(x, y, t) = \nu + \nu'(x, y, t), \tag{5a}$$
$$u(x, y, t) = y + u'(x, y, t), \tag{5b}$$
$$v(x, y, t) = v'(x, y, t), \tag{5c}$$
$$T(x, y, t) = f_2/f_5 + T'(x, y, t). \tag{5d}$$

The dynamics of perturbations is then studied by linearizing the equations of motion around the base flow $(\nu, y, 0, f_2/f_5)$ via the normal-mode analysis,

$$[\nu', u', v', T'](x, y, t) = [\hat{\nu}, \hat{u}, \hat{v}, \hat{T}](y)\, e^{ik_x x + \omega t}. \tag{6}$$

Here k_x is the wavenumber for the x-direction and the quantities with hats are complex amplitudes of perturbations; $\omega = \omega_r + i\omega_i$ is the complex frequency. Instability is associated with positive values of ω_r.

It is known that the uniform granular shear flow is unstable to various kinds of disturbances, leading to both stationary and travelling wave patterns [1]. Here we focus only on a special kind of *stationary* instability that arises due to purely streamwise disturbances $(k_x = 0)$, i.e. the disturbance patterns do not vary with x; we call it *shear-banding instability* since its nonlinear saturation leads to shear-banding-type patterns of alternating bands of dilute and dense regions in the gradient direction. For such disturbances, there is a minimum value of solid fraction $(\nu_{av} \sim 0.15)$ above which the flow is unstable if the Couette gap satisfies the following relation:

$$H \geq n\pi\psi(\nu, e), \tag{7}$$

where $\psi(\nu, e)$ is a complicated function of density and restitution coefficient, and $n = 1, 2, \ldots$ is the mode number (which is related to the eigenfunctions of the linearized stability problem).

It is clear that the $n = 1$ mode is the first to become unstable at a critical value of the Couette gap $H = H_c \equiv \pi\psi(\nu, e)$ (for given ν_{av} and e). Beyond $H > H_c$, the successive higher-order modes $(n = 2, 3, \ldots)$ take over as the most unstable mode at $H = nH_c$.

Treating H as a bifurcation parameter, there is now a countably infinite number of pitchfork bifurcations (since the least-stable eigenvalue is real), located at $H = nH_c$. Before presenting bifurcation results, let us briefly introduce the concept of pitchfork bifurcations by considering the simplest bifurcation problem with one *order* parameter Φ,

$$\frac{d\Phi}{dt} = f(\Phi, \mathcal{B}) = b\Phi^3 - \mathcal{B}\Phi = -f(-\Phi, \mathcal{B}), \tag{8}$$

where $f(\Phi, \mathcal{B})$ is a nonlinear scalar valued function of Φ, $\mathcal{B}$, called the *bifurcation* (*control*) parameter, and b is some real parameter. The bifurcation diagram consists of the set of points in the $(\Phi, \mathcal{B})$-plane which satisfies $f(\Phi, \mathcal{B}) = 0$. For pitchfork (stationary) bifurcations, the number of solutions of $f(\Phi, \mathcal{B}) = 0$ jumps from one to three as the bifurcation parameter $\mathcal{B}$ crosses some critical value $\mathcal{B}_c$. More specifically, the loss of stability of the base solution $\Phi = 0$ gives birth to two *new* solutions,

$$\Phi = \pm\sqrt{\mathcal{B}/b},$$

which are *stable*. These solutions, $\Phi = \pm\sqrt{\mathcal{B}/b}$, are said to be *bifurcated* from the base solution $\Phi = 0$. The bifurcation is called *supercritical* for $b > 0$, and *subcritical* for $b < 0$.
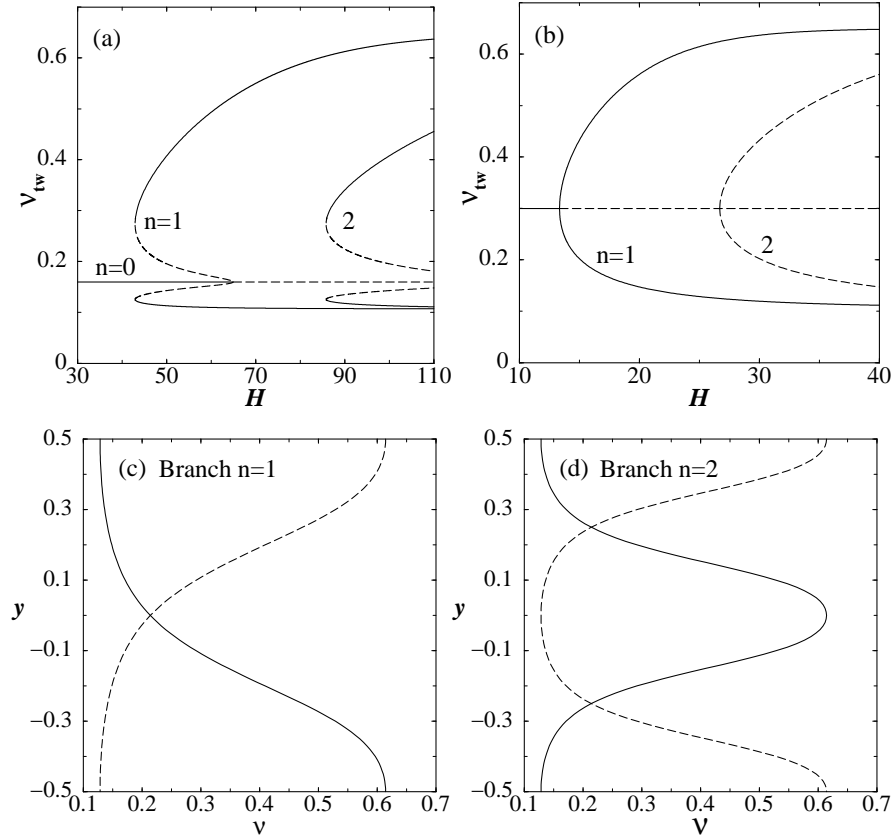

Fig. 2. Evidence of subcritical and supercritical bifurcations in granular Couette flow: the average solid fraction ν_{av} is (**a**) 0.16, (**b**) 0.3; the coefficient of restitution is $e = 0.8$. The *stable* (/*unstable*) bifurcation branch is denoted by solid (dashed) line. (**c-d**) Variations of solid fraction for (**c**) the first-pair ($n = 1$) of solution branches at $H = 25$ and for (**d**) the second-pair ($n = 2$) of solution branches at $H = 50$ with $\nu_{av} = 0.3$; in each panel, the solid and dashed lines represent solutions corresponding to lower and upper bifurcation branches in panel (**b**), respectively

For the present problem, we have chosen the *order* parameter to be $\Phi = \nu(1/2) = \nu_{tw}$, the value of solid fraction at the top-wall, (this can, equivalently, be tied to $(\nu_{tw} - \nu_{av})$ or any other suitable quantity), and the *bifurcation* parameter as $\mathcal{B} = H$ (this can also be tied to $(H - H_c)$, i.e. $\mathcal{B} \equiv \mathcal{B}(H, e, \nu_{av})$). Figure 2(a) shows a typical subcritical bifurcation diagram for the uniform shear case in the (H, ν_{tw})-plane for a low density granular fluid ($\nu_{av} = 0.16$); the coefficient of restitution is $e = 0.8$. The horizontal line refers to uniform shear for which the density is uniform across the Couette gap, i.e. $\nu_{tw} \equiv \nu_{av}$. As we increase the bifurcation parameter H, the uniform shear flow loses stability to the first mode ($n = 1$) at $H = H_c \approx 64.4$ and two *unstable* solution branches emerge from this bifurcation point. Each of these unstable branches eventually turns over at some lower value of $H = H_u \approx 42$ to yield a *stable* solution branch. For the range of Couette gaps $H_u < H < H_c$, there are three possible solutions, with the middle solution branch being unstable. This is an example of *hysteretic* phase transition.

As we increase the average density, the nature of bifurcation changes from *subcritical* to *supercritical* as seen in Fig. 2(*b*) for a moderate density granular fluid ($\nu_{av} = 0.3$). For these parameter combinations, the bifurcation is subcritical for $\nu_{av} < 0.18$ and supercritical for $\nu_{av} > 0.18$. From each bifurcation point, two stable solution branches emerge and such pairs of solutions arise due to the underlying symmetry of the uniform shear flow. Note that all the upper bifurcation branches asymptote to $\nu_{tw} \to 0.65 = \nu_{max}$ which corresponds to the maximum allowable solid fraction in the system, representing the random close-packing limit.

For the sake of completeness, we show the density profiles of the first two branches in Fig. 2(*b*) at $H = 25$ and 50, respectively, in Figs. 2(*c-d*). The solid and dashed lines in Figs. 2(*c-d*) represent solutions belonging to the lower and upper branches of Fig. 2(*b*), respectively. The solutions emerging from $H = H_c, 3H_c, \ldots$ are *asymmetric*, having no symmetry about the centerline ($y = 0$), since the eigenfunctions for odd modes ($n = 1, 3, \ldots$) destroy the center-symmetry (4) of uniform shear. On the other hand, the solutions from $H = 2H_c, 4H_c, \ldots$ are *symmetric* about the centerline, since the eigenfunctions for even modes ($n = 2, 4, \ldots$) satisfy the symmetry (4). Related bifurcation results on the gravity-free uniform shear flow with multiple plugs are detailed elsewhere [11]. In the following, we consider the role of gravity on the fate of such plugged solutions.
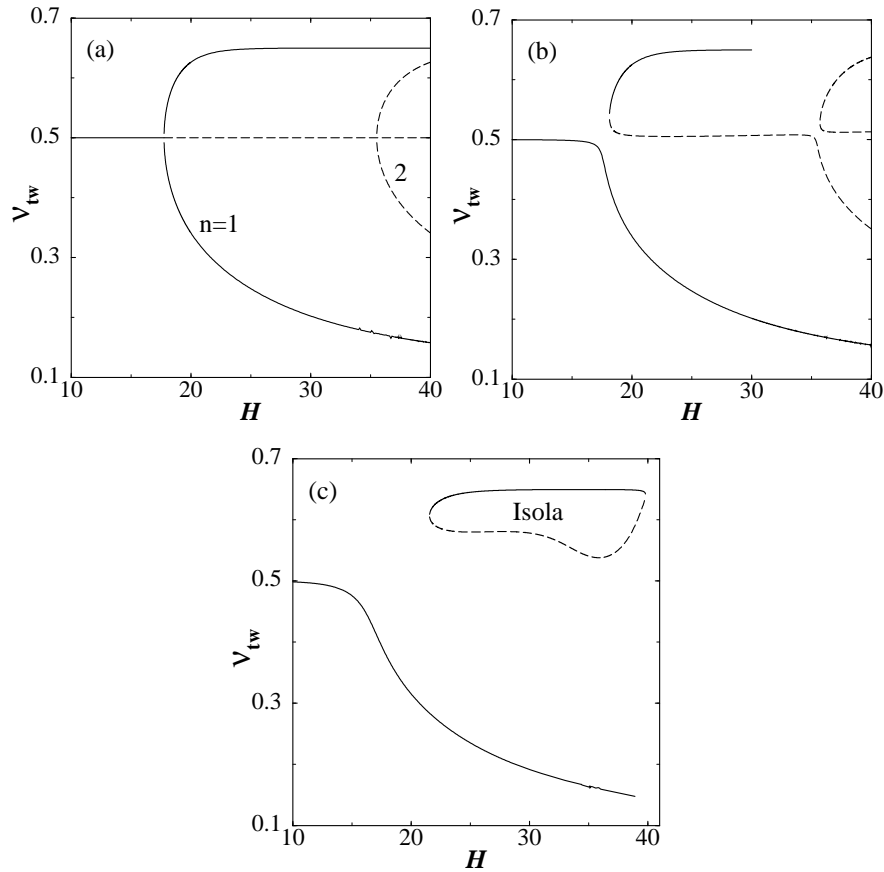

Fig. 3. Effect of gravity on the bifurcation diagram with $\nu_{av} = 0.5$ and $e = 0.8$: (**a**) $Fr^{-1} = 0$; (**b**) $Fr^{-1} = 10^{-3}$; (**c**) $Fr^{-1} = 4 \times 10^{-3}$. The *stable* (*unstable*) bifurcation branch is denoted by solid (dashed) line

4   Gravitational Plane Couette Flow: Gravity as an Imperfection

Figures 3(**a-c**) display three bifurcation diagrams at different Fr^{-1}, showing the effect of gravity on the topology of bifurcations. The average density is set to $\nu_{av} = 0.5$, representing dense flows, and other parameters are as in Fig. 2. For the gravity-free case ($Fr^{-1} = 0$) in Fig. 3(**a**), the topology of bifurcations is similar to that in Fig. 2(*b*). As we increase the gravitational strength to $Fr^{-1} = 10^{-3}$ (Fig. 3*b*), the solution branches from the even and odd modes peels off from each bifurcation point; this is an example of *imperfect* bifurcation. Thus, *gravity acts as an imperfection in the embedded problem*, destroying the bifurcation structure of the gravity-free case. By further increasing the gravitational strength to $Fr^{-1} = 4 \times 10^{-3}$ (Fig. 3*c*), the solution branches are seen to form *isolas*, via merging between two successive bifurcation branches. Interestingly, the size of this isola also decreases with increasing Fr^{-1} which disappears completely at $Fr^{-1} \sim 5 \times 10^{-3}$. This simply implies that gravity does not support the associated solutions. (The sequence of *birth* and *death* of such isolas is detailed elsewhere [4].) The point we want to emphasize is that there is a critical value of Fr ($\sim 5 \times 10^{-3}$ for the parameter combinations of Fig. 3) below which only *one* solution-branch survives in the bifurcation diagram that corresponds to the lower branch of the first mode ($n = 1$) which extends upto $H = \infty$. Note that the density profile corresponding to this 'unique' branch has a plug near the bottom plate as shown by the solid line in Fig. 4*a*.
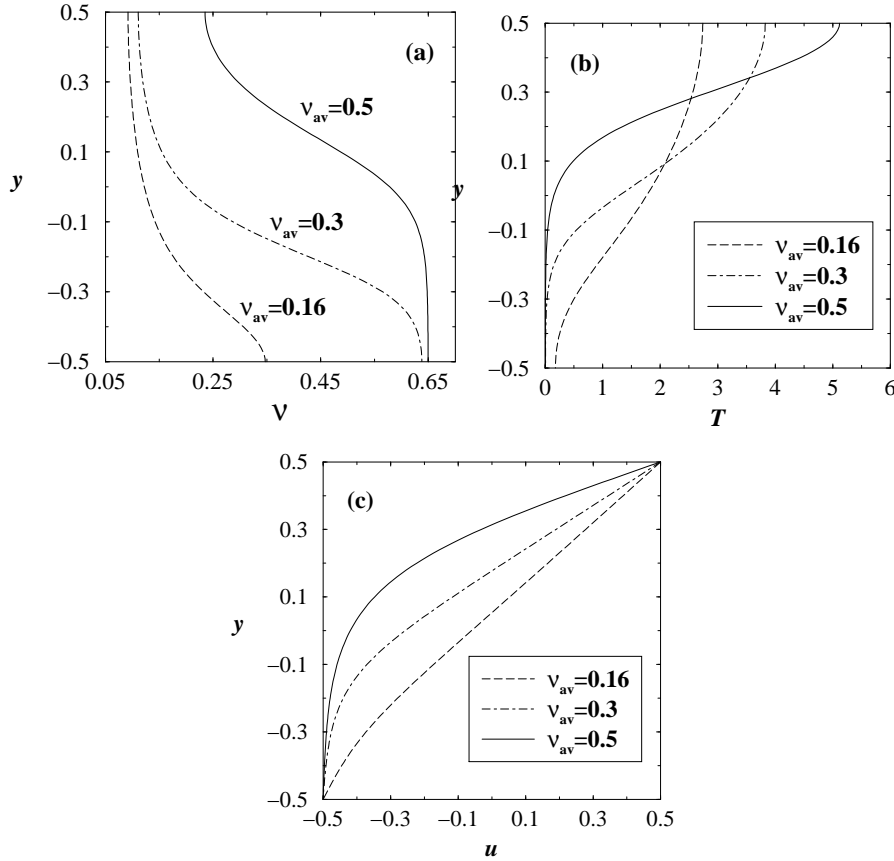

Fig. 4. Effect of average density, ν_{av}, on the profiles of (**a**) volume fraction, (**b**) granular temperature and (**c**) streamwise velocity at $Fr^{-1} = 4 \times 10^{-3}$, $H = 25$ and $e = 0.8$. The solutions correspond to the 'unique' lower bifurcation branch

Figures 4(a-c) show the effect of mean density on the profiles of volume fraction, granular temperature and velocity at $Fr^{-1} = 4 \times 10^{-3}$, $H = 25$ and $e = 0.8$. The dashed, dot-dashed and solid lines represent solutions at $\nu_{av} = 0.16$, 0.3 and 0.5, respectively. We observe that the thickness of the plug increases with increasing ν_{av} and the plug becomes compactified. Within the plug, both the granular temperature and the shear-rate are relatively small. With increasing mean density, the plug becomes almost unsheared (i.e. the local shear rate being close to zero) near the bottom plate.

4.1   Connection with Universal Unfolding of Pitchfork Bifurcation

We have established that gravity acts as an imperfection in the present problem. In the parlance of *singularity* theory [6], the general problem of imperfect bifurcation is addressed by using the theory of 'universal' unfolding which we discuss in this section.
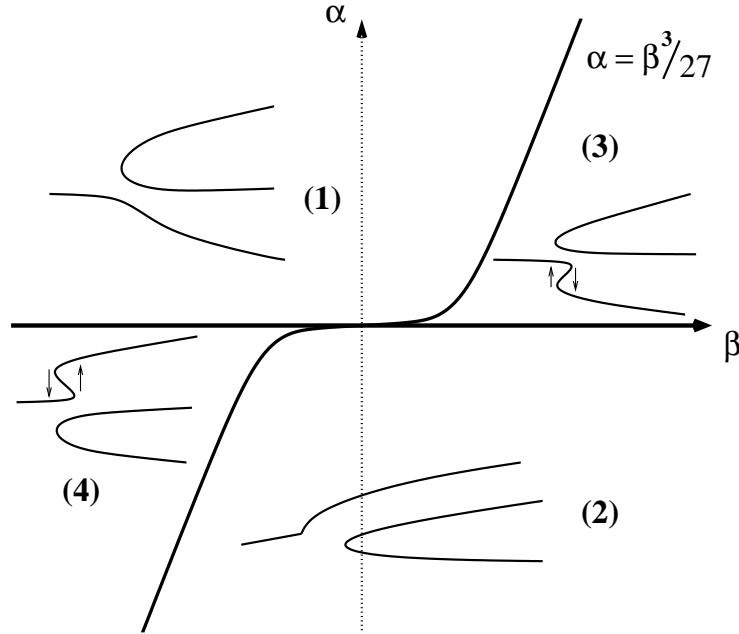

Fig. 5. A schematic phase-diagram for the universal unfolding of pitchfork bifurcations, showing all possible forms of imperfect bifurcations

To connect our bifurcation results with *universal unfoldings*, let us consider the *normal-form* equation for *imperfect* pitchfork bifurcation [6],

$$\frac{\mathrm{d}\Phi}{\mathrm{d}t} = \Phi^3 - \mathcal{B}\Phi + \alpha + \beta\Phi^2 = F(\Phi, \mathcal{B}; \alpha, \beta), \tag{9}$$

where α and β are the imperfection parameters which vanish identically for 'perfect' pitchfork bifurcations such that

$$F(\Phi, \mathcal{B}; 0, 0) \equiv f(\Phi, \mathcal{B}). \tag{10}$$

From the equations of motions, we can assert that these imperfection parameters α and β are functions of Fr, H and ν, i.e.

$$\alpha \equiv \alpha(Fr^{-1}, H, \nu) \tag{11a}$$

$$\beta \equiv \beta(Fr^{-1}, H, \nu), \tag{11b}$$

satisfying the following properties:

$$\alpha(0, H, \nu) = 0 = \beta(0, H, \nu). \tag{12}$$

In fact, one can think of $F(\Phi, \mathcal{B}; \alpha, \beta)$ as a perturbation of the scalar valued function $f(\Phi, \mathcal{B})$. This function $F(\Phi, \mathcal{B}; \alpha, \beta)$ is called the universal unfolding of $f(\Phi, \mathcal{B})$ since it encompasses all possible forms of bifurcation diagrams that can arise due to any form of perturbations on the perfect pitchfork bifurcation.

As discussed in [6], the universal unfolding of the pitchfork leads to four possible bifurcation diagrams in the (α, β)-plane. In particular, two curves $\alpha = 0$ and $\alpha = \beta^3/27$, denoted by thick solid lines in Fig. 5, divide the (α, β)-plane into four zones, and all parameter combinations in each zone represent a canonical bifurcation diagram as shown schematically in this figure. Comparing our bifurcation diagrams in Fig. 3 with these four sets, we find that the bifurcation diagram for zone 1 represents the unfolding of pitchfork bifurcations in our case. However, by redefining our order-parameter as $\Phi = \nu_{bw} \equiv \nu(-1/2)$, i.e. the value of the solid fraction at the bottom wall, and then redrawing the bifurcation diagrams of Fig. 3, we get back the canonical set for zone 2. For this case, the smooth solution branch appears from the upper part of the corresponding $n = 1$ bifurcation branch of the gravity-free case.
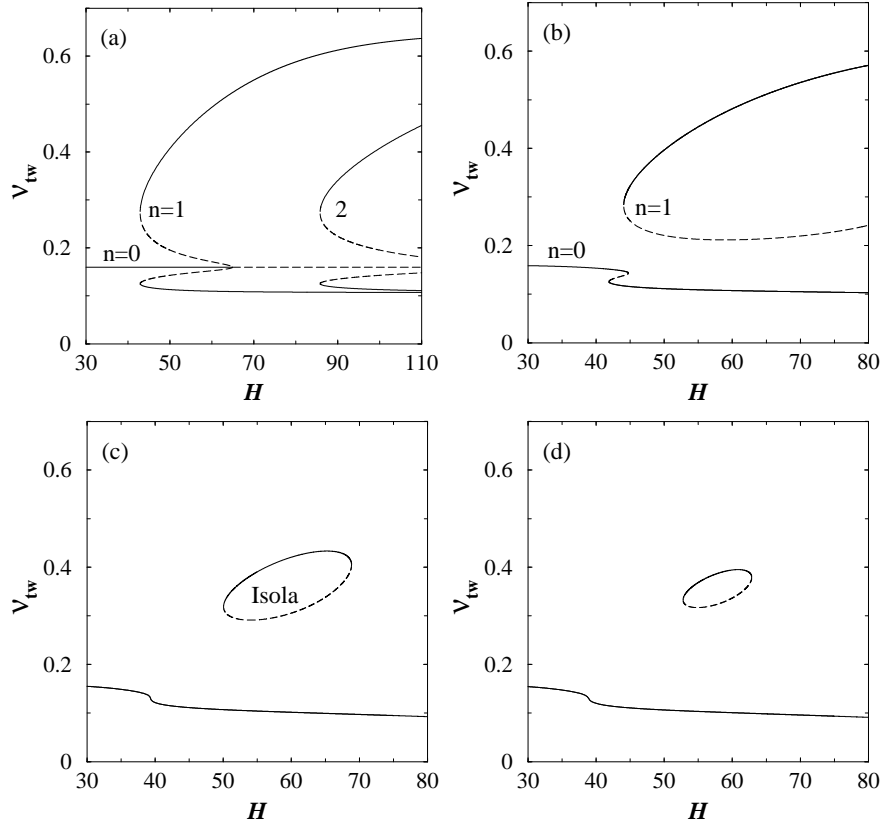

Fig. 6. Effect of gravity on the subcritical bifurcations at $\nu_{av} = 0.16$ and $e = 0.8$: (**a**) $Fr^{-1} = 0$; (**b**) $Fr^{-1} = 2 \times 10^{-4}$; (**c**) $Fr^{-1} = 4 \times 10^{-4}$; (**d**) $Fr^{-1} = 4.25 \times 10^{-4}$. The *stable (unstable)* bifurcation branch is denoted by solid (dashed) line

We have seen that the shear-banding instabilities in granular Couette flow also lead to subcritical pitchfork bifurcations that occur at lower mean densities (cf. Fig. 2a). The

effect of gravity on such subcritical bifurcations is shown in Fig. 6, with parameter values set to $\nu_{av} = 0.16$ and $e = 0.8$. Note that the smooth branch in Fig. 6(b) now contains two *saddle-nodes*, joined by a 'hysteretic' branch; such 'hysteretic' jumps, however, disappear when the gravitational strength is strong (i.e. large Fr^{-1}) as seen in Fig. 6c. From Figs. 6(c) and 6(d) we observe that the size of the isola diminishes with increasing Fr^{-1}, eventually disappearing at $Fr^{-1} \sim 4.4 \times 10^{-4}$ for this parameter combination. Hence, under strong gravitational strength, the surviving attractor in the phase-space is the one that corresponds to a solution with a plug near the bottom wall and a dilute almost uniformly sheared layer near the top-wall.

Returning back to the canonical bifurcation diagrams for universal unfolding in Fig. 5, we observe that the bifurcation diagram for zone 3 is similar to that in Fig. 6(b). Again redefining our order-parameter as $\Phi = \nu_{bw} \equiv \nu(-1/2)$ and then redrawing the bifurcation diagrams of Fig. 6, we get back the canonical set for zone 4. It is now clear that the inclusion of gravity naturally recovers the two 'hysteretic' bifurcation diagrams for zone 3 and zone 4 in Fig. 5. Thus, all possible forms of imperfect bifurcation scenarios can be realized in the present bifurcation problem. We can conclude that the effect of gravity on the granular Couette flow truely belongs to the class of the 'universal' unfolding of pitchfork bifurcations.

4.2   Comparison with Experiments and Discussion

In the regime of dense flows with low shear rates, the experiments and molecular dynamics simulations [13,14] suggest that the shearing mainly occurs in a thin-layer near the top wall, with most of the material remaining almost undeformed near the bottom wall. Recall that in most shear-cell experiments the Froude number is of order 10 (i.e. $Fr^{-1} \sim 0.1$). This is precisely what we have predicted from our analysis: at large values of Fr^{-1} there exists a unique solution with a plug near the bottom wall. Such large values of Fr^{-1} in earth-bound shear-cell experiments clearly preclude the emergence of other solutions that have plugs near the top wall or somewhere in between. Under *micro-gravity* conditions (i.e. at small Fr^{-1}), however, it would be possible to observe such multiple-plugs, 'floating' within the Couette gap. Thus, we can conclude that the gravitational Couette flow admits only one solution, having a plug near the bottom wall and a shear-band near the top wall [2,4]. We have established that the shearband formation in gravitational plane Couette flow is tied to the shearbanding instabilities in 'uniform shear flow' via the route of the universal unfolding of pitchfork bifurcations.

Acknowledgements

References

1. M. Alam, P.R. Nott: Stability of plane Couette flow of a granular material. J. Fluid Mech. **377**, 99–136 (1998)

2. M. Alam: The role of gravity on granular shear flow: steady flow, bifurcation and stability. Bull. Am. Phys. Soc. **43**, 2009 (1998)

3. M. Alam, S. Luding: First normal stress difference and crystallization in a dense sheared granular fluid. Phys. Fluids **15**, 2298-2312 (2003)

4. M. Alam, V.H. Arakeri, P.R. Nott, D. Godard, H.J. Herrmann: Instability-induced ordering, universal unfolding and the role of gravity in granular Couette flow. J. Fluid Mech. (2004, In press).

5. H. J. Herrmann, J.-P. Hovi, S. Luding: *Physics of Dry Granular Media.* 1st edn. (Kluwer Academic, Holland 1998)

6. M. Golubitsky, D. Schaeffer: *Singularities and Groups in Bifurcation Theory* **I**. 1st edn. (Springer, New York 1985)

7. K. Hutter, K.R. Rajagopal: On flows of granular materials. Continuum Mech. Thermodyn. **6**, 81-139 (1994)

8. S. Luding: Clustering instabilities, arching, and anomalous interaction probabilities as examples for cooperative phenomena in dry granular media. T.A.S.K. Quarterly **2**, 417-443 (1998)

9. S. Luding: Structures and non-equilibrium dynamics in granular media. Comptes Rendus Academic des Sciences **3**, 1-9 (2002)

10. C.K.K. Lun, S.B. Savage, D.J. Jeffrey: Kinetic theories for granular flow: inelastic particles in Couette flow and slightly inelastic particles in a general flow field. J. Fluid Mech. **140**, 223-245 (1984)

11. P.R. Nott, M. Alam, K. Agrawal, R. Jackson, S. Sundarsan: The effect of boundaries on the plane Couette flow of granular materials: a bifurcation analysis. J. Fluid Mech. **397**, 203–229 (1999)

12. S.B. Savage: Instability of unbounded uniform granular shear flow. J. Fluid Mech. **241**, 212–233 (1992)

13. S.B. Savage, M. Sayed: Stresses developed by dry cohesionless granular materials sheared in an annular shear cell. J. Fluid Mech. **142**, 391–425 (1984)

14. P.A. Thomson, G. Grest: Granular flow: friction and the dilatancy transition. Phys. Rev. Lett. **67**, 1751–1754 (1991)